The Effects of Filtration on Pressure Drop and Energy Consumption in Residential HVAC Systems (RP-1299)

Brent Stephens Student Member ASHRAE
Atila Novoselac, PhD Associate Member ASHRAE
Jeffrey A. Siegel, PhD Member ASHRAE

Received August 4, 2009; accepted December 15, 2009

This paper is based on findings resulting from ASHRAE Research Project RP-1299.

The use of high-efficiency HVAC filters is a common strategy to control exposure to airborne particulate matter in residential buildings. However, high-efficiency filters generally have a higher pressure drop and are widely assumed to have large energy penalties. In this paper, we explore the underlying theoretical energy implications of high-pressure-drop filters and we present the results of a four-month-long period of detailed energy monitoring of two air-conditioning systems in a test home in Austin, Texas. A theoretical analysis shows that the magnitude of potential energy impacts associated with high-efficiency filters are overall likely to be small and can result in either a net savings or additional expenditure, depending on the system. The measured results in the test systems confirm these findings, and energy consumption generally did not differ with high-efficiency filters compared to low-efficiency filters. These results suggest caution when assuming that high-efficiency filters require more energy than low-pressure-drop filters in residential HVAC systems.

INTRODUCTION

High-efficiency filters are used in forced-air heating, ventilating, and air-conditioning (HVAC) systems to protect building equipment and occupants, but are also known to influence HVAC energy consumption. High-efficiency filters with a high minimum efficiency reporting value (MERV) typically have a greater pressure drop than a filter with a lower MERV (ASHRAE 2007). In large commercial HVAC systems, where fan and motor controls typically maintain required airflow rates, a greater pressure drop will generally lead to increased energy consumption (e.g., Chimack and Sellers [2000], Fisk et al. [2002], and Yang et al. [2007]). This relationship between energy use and filter pressure drop is widely assumed to hold true for smaller residential air-conditioning systems, but operational differences between small and large systems suggest very different energy consequences. This paper explores the theoretical impacts of filters on smaller air-conditioning systems and reports measurements taken with different levels of filter efficiency installed in an unoccupied test house in Austin, Texas, during the cooling season. This paper is a companion paper to similar measurements taken on 17 HVAC systems in occupied residential and light-commercial buildings (Stephens et al. 2010).

Brent Stephens is a graduate research assistant, **Atila Novoselac** is an assistant professor, and **Jeffrey Siegel** is an associate professor in the Department of Civil, Architectural, and Environmental Engineering at the University of Texas at Austin.

BACKGROUND

Over 70% of residential buildings in the United States use central forced-air distribution systems for heating and air-conditioning purposes (HUD 2005). Most residential cooling systems are direct expansion (DX) systems with the condenser and compressor located outside of the building envelope. The air-handling unit (AHU) is usually positioned either inside the building envelope (e.g., closet or conditioned attic) or outside of conditioned space (e.g., vented attic or garage). Residential HVAC systems usually use supply distribution ducts to provide cooling and heating throughout the building. Systems typically have either return ducts or a direct intake from the conditioned space, depending on the configuration of the house and the location of the AHU. Most existing residential systems in the United States do not incorporate dedicated outdoor air ventilation (e.g., Chan et al. [2005], Sherman [2008], and Waring and Siegel [2008]). Air filters are typically installed in the return airstream at either the AHU or the return duct grille(s). The configuration of supply ducts, return ducts, supply registers, and return grilles, along with the position of individual components within the AHU (i.e., filter, fan, cooling coil, and heating coils/heat exchanger) can vary and can affect the pressure distribution throughout the system.

Figure 1 presents a typical configuration of an AHU with both return and supply ducts and the corresponding pressure distribution in the system. It illustrates the change of static pressure due to airflow across the different components of the system. The magnitude of total static pressure that the AHU fan must overcome is generally less than 250 Pa (1 in. w.c.) in residential systems (ASHRAE 2004a; Proctor and Parker 2000). Almost all of the pressure potential is used to overcome friction introduced by different components of the system, outlined in Figure 1a. Figure 1b shows the static pressure distribution relative to the surrounding pressure in the occupied residence space.

The static pressure drop across individual components of the system is proportional to the square of the airflow rate and a coefficient of proportionality, C (ASHRAE 2005). There are some component installations where either a combination of a linear and a squared term or an empirically derived exponent is used (e.g., Yang et al. [2007]), but we focus on the classic form

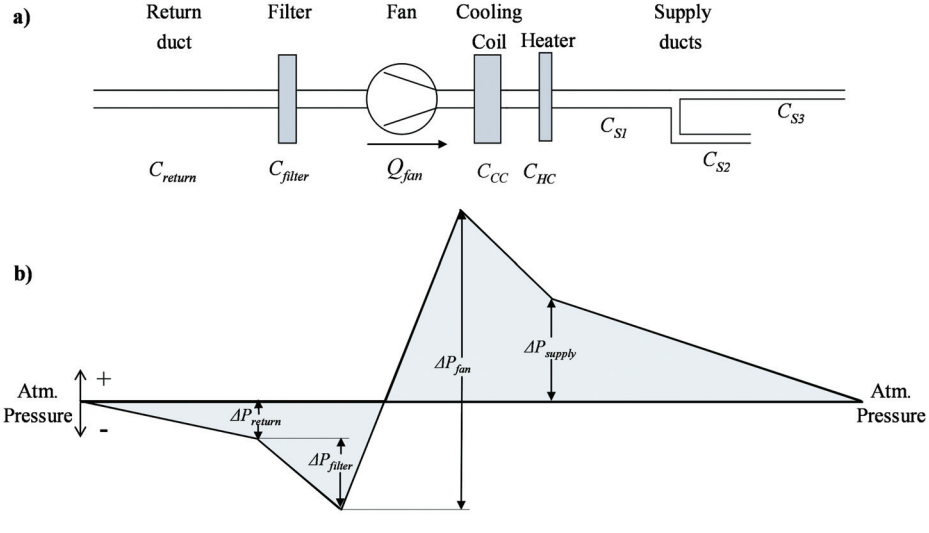

Figure 1. Pressure distribution in a residential HVAC system: (a) system schematic, (b) static pressure distribution.

here. The coefficient, C, depends on component geometries and is constant for static system components such as return grilles, supply registers, ducts, and heating coils. The coefficient for a filter can increase as the filter becomes loaded over time and the pressure drop is increased. Similarly, the coefficient of proportionality for the cooling coil can also change as the moisture from air condenses on the surfaces, changing the geometry. However, this study considers only the effects of filter pressure drop on system operation.

Figure 1a illustrates that residential HVAC systems can be presented as systems of components connected in series, with duct branches connected in parallel (note that only two supply duct branches are shown for simplicity; more usually exist in real systems). Equation 1 represents the combination of the component coefficients in Figure 1a, resulting in a total equivalent coefficient of proportionality for the entire system, C_{total}.

$$C_{total} = C_{return} + C_{filter} + C_{CC} + C_{HC} + C_{S1} + \frac{C_{S2} + C_{S3}}{C_{S2} \cdot C_{S3}} \quad (1)$$

where

C_{total} = coefficient of proportionality for the entire system
C_{return} = coefficient of proportionality for the return duct
C_{filter} = coefficient of proportionality for the filter
C_{CC} = coefficient of proportionality for the cooling coil
C_{HC} = coefficient of proportionality for the heating coil
C_{S1} = coefficient of proportionality for the first supply duct branch
C_{S2} = coefficient of proportionality for the second supply duct branch
C_{S3} = coefficient of proportionality for the third supply duct branch

Since the pressure loss in each component can be presented as a square function of airflow through the component and the geometry of all components remains constant (excluding the filter), the required pressure increase across the system fan, ΔP_{fan}, can be expressed as a function of the airflow rate, Q_{fan}, and C_{total}, as shown in Equation 2.

$$\Delta P_{fan} = C_{total} \cdot Q_{fan}^2 = (C_{filter} + C_{system}) \cdot Q_{fan}^2 \quad (2)$$

where

ΔP_{fan} = required pressure increase across the fan
Q_{fan} = system airflow rate
C_{system} = coefficient of proportionality for the system, excluding the filter

The filter coefficient, C_{filter}, changes with both filter efficiency and time as it loads. The filter coefficient and system coefficient, C_{system}, can be used to express the contribution of the filter on total pressure drop in a system ($C_{filter} / [C_{filter} + C_{system}]$). The contribution of the filter to total system pressure drop is usually in the range of 20%–50% and depends on the system configuration, filter efficiency (MERV), and loading condition (Stephens et al. 2010).

High-efficiency or high-pressure-drop filters can influence energy use in three primary areas of residential HVAC systems: (1) the AHU fan, (2) the outdoor compressor unit, and (3) duct leakage. Each of these impacts is explored below.

Fan Impacts. The power draw of an AHU fan can be described as a function of the required pressure increase across the fan and the airflow rate, as shown in Equation 3 (ASHRAE 2004b).

$$W_{fan} = \frac{\Delta P_{fan} \cdot Q_{fan}}{\eta_{fan} \cdot \eta_{motor}} = \frac{C_{total} \cdot Q_{fan}^3}{\eta_{fan} \cdot \eta_{motor}} = \frac{(C_{filter} + C_{system}) \cdot Q_{fan}^3}{\eta_{fan} \cdot \eta_{motor}} \quad (3)$$

where

W_{fan} = power draw of fan
η_{fan} = efficiency of the fan
η_{motor} = efficiency of the fan motor

In HVAC systems where airflow remains constant by the use of variable-speed fans and the efficiencies of the fan shaft and motor do not change with the airflow rate, the power draw of the fan is a linear function of the filter coefficient. Equation 3 indicates that, in this case, a 10% increase in total pressure drop would cause a 10% increase in fan electric power draw. However, most residential HVAC systems use permanent split capacitor (PSC) air-handler fan motors that do not have controls to keep airflow rates constant, and an increase of filter pressure drop will generally decrease the airflow rate (Parker et al. 1997; Stephens et al. 2010).

Pressure and flow relationships for HVAC systems and fans can be characterized by system and fan curves, as shown in Figure 2. In this theoretical example of a typical HVAC system without flow controls, replacing the mid-MERV filter with a high-MERV filter (i.e., increasing the filter pressure drop) increases the total system pressure and decreases the airflow rate, as the working point moves from point A to point B. The reverse effect occurs when decreasing the filter efficiency or pressure drop (moving from point A to point C in Figure 2).

In the theoretical example in Figure 2, if a high-efficiency filter increases total system pressure by approximately 40%, the working point moves from point C to point B, and airflow decreases approximately 30%. When the working point is along the concave part of the fan curve (such as point B in Figure 2), the magnitude of a decrease in airflow is greater than the magnitude of an increase in pressure, and the energy delivered to the air (the product of $\Delta P_{fan} \cdot Q_{fan}$) decreases as ΔP_{fan} increases. When the working point is along the linear part of the fan curve (such as point C in Figure 2), the energy delivered to the air remains constant as long as a pressure increase or decrease keeps the working point within the linear range. The effect

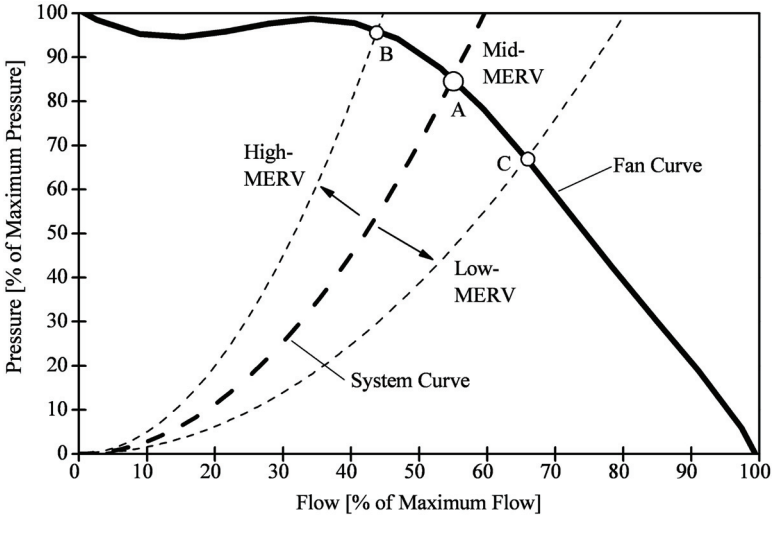

Figure 2. System and fan curves for medium-, high-, and low-pressure-drop filters.

that airflow changes have on fan power draw depends on the magnitude of pressure drop, airflow, and fan and motor efficiencies shown in Equation 3.

Fan shaft efficiency, which defines the ratio of shaft torque that is converted to airflow, typically peaks in the central region of the airflow range and is generally lower at the high and low bounds of airflow rates. Fan motor efficiency, which defines the input energy that the motor converts to useful shaft torque, typically increases with the power delivered to the shaft. Peak fan efficiencies in residential systems are generally less than 70%, and peak motor efficiencies are generally between 30%–70%, respectively (Sachs et al. 2002). Figures 3a and 3b show pressure, efficiency, and power curves for two different fan types to illustrate how the shape of fan efficiency curves affects the fan power draw. Points A, B, and C provide theoretical working points for different pressure drop filters.

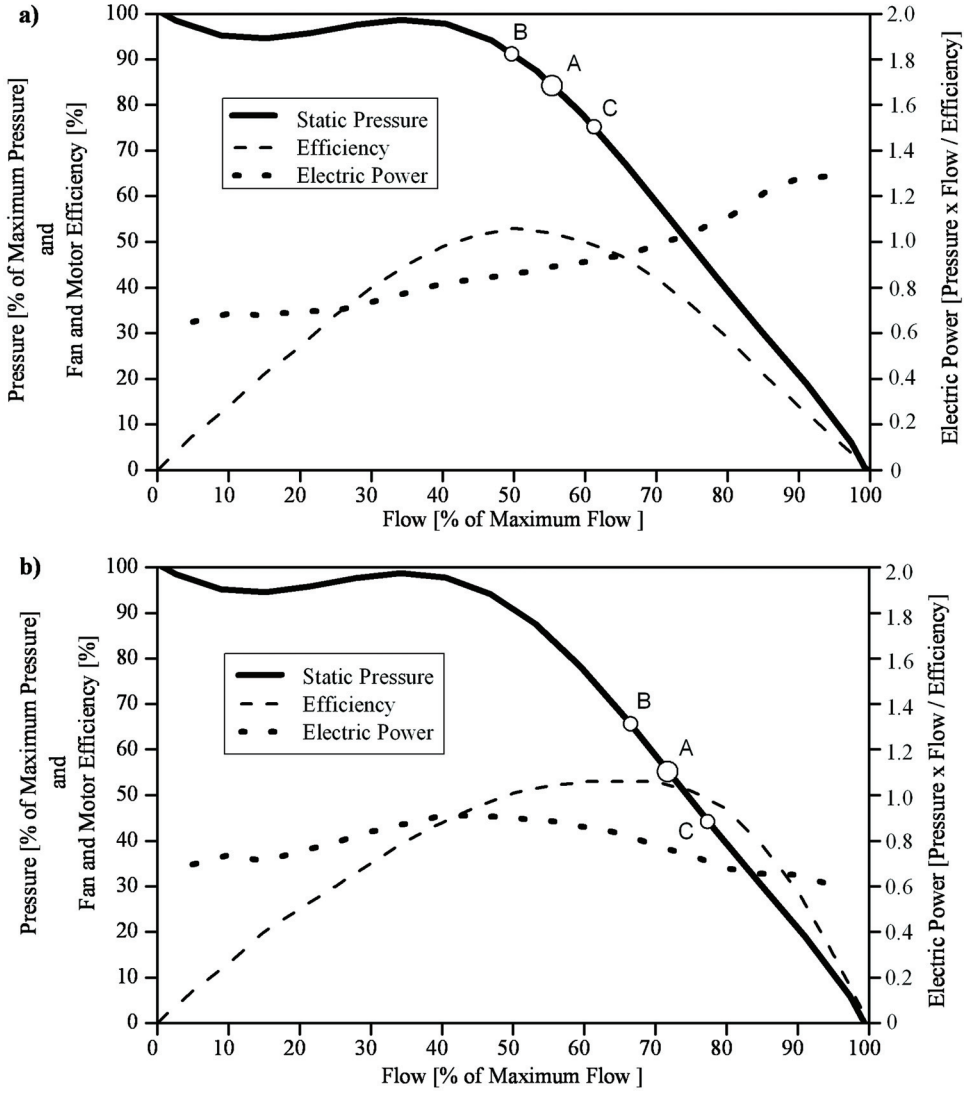

Figure 3. Fan pressure, power, and efficiency curves for (a) airfoil fans and (b) forward-curved low-pressure residential fans.

For the airfoil fan represented in Figure 3a, a 10% increase in total pressure drop due to changing filters and moving from point A to point B would decrease airflow approximately 12%, and decrease fan power draw approximately 8%. For the forward-curved fan represented in Figure 3b, a 20% increase in pressure drop from point A to point B would decrease airflow approximately 7%, and fan power draw would actually increase approximately 7%. Again, these working points are hypothetical points on two representative fan curves and do not represent actual measured values. However, they show the impact that the shape of the fan efficiency curve and the change in working point on the fan curve due to filters can have on fan power draw.

The fan and motor efficiency curves depend on the type of fan design, the properties of the electric motor, and the installation position of the fan in the AHU. Most residential units have sheet metal centrifugal fans with thin, forward-curved impeller blades that have a low maximum efficiency, and approximately 90% of residential fans have permanent split capacitor (PSC) motors (Sachs et al. 2002). Alternative fan designs can include electronically commutated DC permanent magnet motors (ECM) whose pressure and flow relationships will behave differently than PSC motors, but they currently have a limited market share in residential systems.

Outdoor Condenser Unit Impacts. The effects of high-pressure-drop filters on the operation of outdoor condenser units are not well known, but diminished airflow across the cooling coil is known to affect (1) heat transfer on the surface of the cooling coil, (2) the refrigerant evaporation process within the cooling coil, and (3) compressor operation. Reduced airflow due to filters can influence the cooling capacity and overall energy consumption of DX cooling systems.

Heat transfer on the surface of the cooling coil defines how much sensible and latent energy the coil removes from the airstream. Reduced airflow will generally reduce convective heat transfer of sensible energy from the air to the surface of the cooling coil, which will decrease sensible cooling capacity; however, this can lead to a lower cooling coil surface temperature and increase moisture removal capability. A lower airflow rate also enables a longer contact time between the air and coil surface area, which further increases dehumidification capacity. Because of these interacting effects, the magnitude of total cooling capacity reduction does not directly follow the magnitude of airflow reduction.

A decrease in cooling capacity can affect the refrigerant evaporation pressure and the refrigerant flow rate through the cooling coil. The impact depends on the type of expansion valve. In residential DX systems with a thermostatic expansion valve (TXV), the refrigerant flow rate will vary with cooling capacity because the valve will control the flow of liquid refrigerant entering the evaporator to maintain the refrigerant vapor at the exit of the cooling coil at a relatively constant temperature and pressure. In residential DX systems with a capillary tube or orifice expansion valve, the evaporation pressure and temperature will vary with cooling capacity. Therefore, a decrease in cooling capacity will cause a lower evaporation pressure and potentially reduce the refrigerant flow rate. In systems with a TXV, a reduction of cooling capacity will not change the refrigeration efficiency considerably since the evaporation pressure does not change and the reduced refrigerant flow reduces the power draw of the compressor. In a DX system with a capillary tube or orifice expansion valve, a reduction in cooling capacity can decrease the efficiency of the cooling cycle, but the power draw of the compressor may also decrease due to the reduced refrigerant flow rate.

Compounding refrigerant charge effects, the power draw, and overall energy consumption of the outdoor unit also depends on the length of compressor operation and refrigerant charge. Most residential systems often operate at non-ideal unsteady-state conditions, and the effects are less well known. Most residential systems are either undercharged or overcharged (Downey and

Proctor 2002) and, thus, the effects of reduced airflow with high-efficiency filters at these non-ideal conditions are far less predictable by these theoretical considerations.

Using experimental measurements and simulations, researchers have shown that the net effect of low airflow is a decrease in cooling system efficiency because cooling capacity generally decreases more than the compressor power draw. For example, Rodriguez et al. (1996) showed that in air-conditioner tests with an orifice expansion valve, a 10% reduction in airflow caused capacity to decrease by approximately 7%, power draw to decrease by less than 1%, and COP to decrease by approximately 6%. Reductions in capacity, power draw, and COP were approximately 10%, 1%, and 8%, respectively, with a 20% airflow rate reduction.

Duct Leakage Impacts. Many residential duct systems are located partially or entirely outside of conditioned space, and duct leaks (both conductive and convective) can have a significant energy penalty. Supply-side leaks can lead to a direct energy penalty as conditioned air is lost to the outside of a building. Return-side leaks can lead to increased sensible and latent loads and diminished air-conditioning system effectiveness (e.g., Siegel et al. [2000], O'Neal et al. [2002], and Francisco et al. [2006]). Since most residences do not incorporate dedicated outdoor air ventilation, duct leakage can also be a primary source of air infiltration or exfiltration.

Because residential systems do not operate at a fixed pressure drop, an increased filter pressure drop can change return- and supply-side duct leakage by altering the pressure distribution in the duct system. The direction and magnitude of the impact on duct leakage due to changes in flow and pressure drop depends on the locations of the filter and the leaks. Increasing the pressure drop of a filter located at the air handler may cause lower return system pressure differences between the return grille and the filter because more of the total pressure drop occurs near the air handler, which can lead to decreased return duct leakage. Conversely, an increase of the pressure drop of a filter at the return grille(s) in a system, such as the one in Figure 4, can lead to increased return system leakage because the pressure differential between the air in the return duct and the surrounding air can increase. Changes in pressure distribution will not necessarily occur uniformly throughout all the branches of ductwork, so individual rooms are subject to pressure imbalances, which affect infiltration loads and supply air delivery. An important aspect of duct leakage is that system impacts generally scale with the leakage fractions, defined as duct leakage divided by system airflow (ASHRAE 2004c). Because airflow

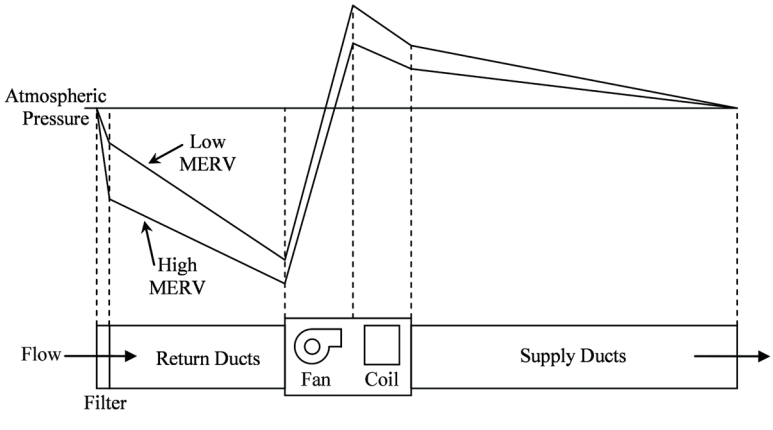

Figure 4. Example static pressure distribution for a residential system.

also generally diminishes with a high-efficiency filter, this can serve to enhance or diminish any duct leakage impacts.

Summarizing the previous sections, the airflow and energy consequences of a high-pressure-drop filter in residential HVAC systems depend on the pressure drop of the filter relative to that of the rest of the return side of the system, the system fan curve, the fan-efficiency curve, and the location of the intersection of the fan and duct curves. In general, the underlying theory, in conjunction with values from literature, suggests that the energy effects of high-efficiency filters in residential systems are likely small. In residential air-conditioner field tests, Parker et al. (1997) measured a 4%–5% airflow rate reduction when replacing standard disposable filters with high-efficiency pleated filters. In four previous studies, a 5%–10% reduction from recommended airflow rates (the range of airflow reductions most likely due to filters) has been shown to diminish total capacity, sensible capacity, and system efficiency by approximately 1%–6%, increase latent capacity by approximately 1%–3%, and diminish total power draw (fan + outdoor unit) by less than 1% (Palani et al. 1992; Rodriguez et al. 1996; Parker et al. 1997; Kim et al. 2009). The magnitude of the effects of filters on duct leakage, total power draw, and cooling capacity are not well characterized. We know of no direct research on the implications of filtration on duct leakage, but a small decrease in duct leakage could have potentially large energy benefits, as capacity delivered to registers has been shown to increase 4%–8% with a small 3% decrease in duct leakage (Walker et al. 1998).

To support the theoretical analysis and experimentally investigate the energy consequences of high-efficiency filters, we monitored two residential air-conditioning systems in an unoccupied test house on a research campus in Austin, Texas. First, we experimentally developed fan curves for the two systems. Second, we made continuous measurements of system airflow, power draw, cooling capacity, pressure drops across filters and coils, and supply duct leakage with low-, medium-, and high-efficiency filters installed over a period of seven months, although refrigerant charge and fan-speed changes limit the available data to four months.

METHODOLOGY

The next section details the test house systems and monitoring equipment, the fan curve determination experiment, and the continuous measurements made with different filtration efficiencies installed.

Test House Equipment Description

An unoccupied manufactured home served as a controlled test site. The home contained two 2.5 ton (8.8 kW) air-conditioning systems that were continuously monitored. The indoor AHUs were identical with identical PSC motors, but one system was installed in an upflow configuration, supplying air from ceiling diffusers, and the other was installed in a downflow configuration, supplying air from floor registers. The outdoor unit matched with the down-flowing system was a heat pump, while the upflow outdoor unit had only cooling capabilities. Both systems had 15 kW (51 kBtu/h) electrical resistance heaters installed in the AHU. Neither unit had return ductwork, but supply ductwork for both units was located in unconditioned spaces—in the attic for the upflow unit and in the crawlspace for the downflow unit.

Continental Control Systems (CCS) Wattnode AC true power meters were installed at each air-handler fan and outdoor unit and connected to 0–20 A CCS current transducers. The power meters were connected to an Onset HOBO Energy Logger Pro. An Energy Conservatory Automated Performance Testing (APT) System was connected to pressure taps, temperature sensors, and relative humidity sensors. Pressure taps were installed before and after the filter, before and after the coil, and in the supply plenum on both air handlers. Indoor temperature and

relative humidity sensors were installed before the filter and after the coil in both systems. Outdoor temperature and relative humidity measurements were made with a HOBO U12 datalogger. Airflow and duct leakage tests were conducted using an Energy Conservatory Duct Blaster and Model 3 Blower Door in accordance with ANSI/ASHRAE Standard 152 (ASHRAE 2004c). System airflow was measured with an Energy Conservatory TrueFlow metering plate and DG-700 digital manometer. The manufacturer reported accuracies for each piece of equipment are listed in Table 1.

Fan Curve Determination Procedure

A series of experiments were conducted to establish fan curves and to characterize fan power draw and flow relationships for both systems in the test house. The procedure involved switching the systems to fan-only operation at the thermostat, blocking the filter slot with a solid plate, and holding it in place in varying positions to simulate an alteration in filter pressure drop. Airflow, fan power draw, filter pressure drop, coil pressure drop, and supply plenum operating pressure were measured and averaged at each simulated filter pressure drop condition. The total system pressure overcome by the AHU fan was calculated as the sum of filter pressure drop, coil pressure drop, and supply plenum operating pressure drop.

Table 1. Test House Instrumentation

Measurement	Units	Equipment	Accuracy
Logged Measurements			
Pressure	Pa (in. w.c.)	Energy Conservatory Automatic Performance Testing System	±1% of reading
Power draw	V	CCS Wattnode	±0.45% of reading and ±0.05% FS
	A	CCS Current Transducer	±1% of reading
	W	Onset Energy Logger Pro	±1.5%[1]
Temperature	°C (°F)	Energy Conservatory precision NTC thermistor	±0.25°C (±0.45°F) from 0°C–75°C (32°F–167°F)
Relative humidity	%	Energy Conservatory thermostet polymer based capacitance sensor	±5% from 0%–90% RH; ±8% at 90% RH
Periodic Measurements			
Pressure	Pa (in. w.c.)	Energy Conservatory DG-700	±1% of reading or 0.15 Pa (0.0006 in. w.c.)
Airflow	m^3/h (cfm)	Energy Conservatory TrueFlow Plate	±7% of reading[2]
Duct leakage	m^3/h (cfm)	Energy Conservatory Duct Blaster	±3% of reading or ±2 m^3/h (±1 cfm)

[1] Voltage and amperage accuracies added in quadrature produced an uncertainty of ±1.2% in the power draw measurements. The estimated uncertainty was rounded to ±1.5% for use in this study because of unknown uncertainties associated with higher-order harmonics.

[2] Manufacturer's literature reports 7%, but conversations with the manufacturer suggest that a higher accuracy is appropriate for repeated measurements of flow differences, which led to the 5% uncertainty determination used in this work.

Continuous Measurements

The two test systems were continuously monitored between July 2008 and November 2008, and three levels of readily available 1 in. (25.4 mm) filters were installed: low-efficiency fiberglass panel filters (MERV < 4), medium-efficiency synthetic pleated filters (MERV 8), and high-efficiency synthetic pleated filters (MERV 11). Filter efficiencies are as reported by the manufacturer. The useful testing periods for low-MERV, mid-MERV, and high-MERV filters during the cooling season were approximately 7 weeks, 2 weeks, and 7 weeks, respectively. During the test periods, all dataloggers were synchronized to record continuously at 10-second intervals. Outdoor temperature and relative humidity measurements were made at 15-minute intervals. The system fans operated continuously, and programmable thermostats were kept at consistent schedules throughout the test periods. The thermostats alternated the daily times of operation of each unit so that they were never competing to meet the cooling load. Estimates of supply duct leakage were assessed at each collected data point by correcting for changes in the observed supply plenum operating pressure and using a power-law flow-leakage approximation following the procedures in the Duct Blaster manual and ANSI/ASHRAE Standard 152-2004, as shown in Equation 4 (ASHRAE 2004c; The Energy Conservatory 2007).

$$Q_{leak} = C\left(\frac{\Delta P}{2}\right)^{n} \tag{4}$$

where

Q_{leak} = operating volumetric leakage flow rate of air, m^3/h (cfm)
ΔP = pressure difference between supply plenum and outside of duct system, Pa
C = coefficient of duct leakage curve, $(m^3/h)/Pa^n$ (cfm/Pa^n)
n = exponent of duct leakage curve, dimensionless

Estimates of airflow were assessed at each data point based on corrections in the measured supply plenum operating pressure, following the calculation procedure in the TrueFlow Manual and ANSI/ASHRAE Standard 152-2004, as shown in Equation 5 (ASHRAE 2004c; The Energy Conservatory 2006).

$$Q_{fan} = Q_{reference}\sqrt{\frac{\Delta P_{operating}}{\Delta P_{reference}}} \tag{5}$$

where

$Q_{reference}$ = volumetric flow rate of air with measuring device installed, m^3/h (cfm)
$\Delta P_{reference}$ = supply plenum pressure with measuring device installed, Pa (in. w.c.)
$\Delta P_{operating}$ = operating supply plenum pressure, Pa (in. w.c.)

Previous field studies have relied on the metrics of sensible capacity, latent capacity, and coefficient of performance (i.e., system efficiency) in attempt to address the complicated relationship between airflow, system runtime, and overall energy consumption (e.g., Parker et al. [1997]). We used the same metrics to describe the cooling performance of the systems using the measured data with different levels of filtration efficiency. The total capacity, q_t (W, Btu/h), calculation is shown in Equation 6. The first term defines sensible capacity and the second term defines latent capacity.

$$q_t = Q_{fan}\rho(C\Delta T + \Delta W h_{fg}) \tag{6}$$

where

Q_{fan} = volumetric flow rate of air flowing through the cooling coil, m^3/s (ft^3/h)
ρ = air density, assumed constant, 1.2 kg/m^3 (0.075 lb_m/ft^3)
C = specific heat of air, assumed constant, 1.005 kJ/(kgK), (0.24 Btu/[lb_m°F])
ΔT = temperature difference across the cooling coil, K (°F)
ΔW = humidity ratio difference across the cooling coil, kg/kg (lb_m/lb_m)
h_{fg} = latent heat of vaporization for water, assumed constant, 2257 kJ/kg (970 Btu/lb)

The coefficient of performance, COP (or energy efficiency ratio, EER), calculation is shown in Equation 7 (COP: W/W = dimensionless; EER: (Btu/h)/W).

$$\text{COP, EER} = \frac{q_t}{W_{ou} + W_{fan}} \tag{7}$$

where

W_{ou} = power draw of the outdoor unit, including the compressor, W
W_{fan} = fan power draw, W

The cooling capacities were analyzed during the recorded cycles only when the systems reached a period of steady-state operation. Measured observations were flagged in the analysis as steady state when the supply plenum temperature did not vary for a period of at least 2 min by more than 0.5°C (0.9°F) from the lowest temperature recorded during a cycle.

Although the capacity and efficiency calculations in Equations 6 and 7 assess the cooling performance of a system, little is known about how changes in sensible capacity actually translate to thermostat readings to ultimately affect runtime and energy consumption. To address this, we also measured the daily electrical energy consumption and runtime of the test systems. The amount of energy consumed during the day by the air conditioner, E (kWh), is defined in Equation 8 as the sum of the energy consumed during all of the cycles throughout the 24 hours in a day. The energy consumption during each cycle is defined as the total power draw of each cycle times the length of a cycle, l_{cyc}.

$$E = \sum_{t=0}^{t=24} (W_{ou} + W_{fan})_{cyc} \cdot l_{cyc} \tag{8}$$

where

t = hour of the day
l_{cyc} = length of an air-conditioning cycle, hours
E = daily energy consumption of the air conditioner, kWh

Outdoor temperature and evaporator entering wet-bulb temperature are two conditions that are known to affect capacity, power draw, and system runtime. In real systems, thermostat settings by occupants are behavioral parameters that affect air-conditioner energy consumption as well. However, since the test house was unoccupied and programmable thermostats kept temperature setpoints constant throughout the test period, we were able to limit the confounding factors to climatic conditions alone. Accordingly, a binned analysis was conducted to isolate climatic effects from those possibly attributed to changes in filter MERV categories. The binned analysis compared data at 32 size ranges of similar outdoor dry-bulb and indoor-entering wet-bulb conditions. The bins are described in Table 2.

In the binned analysis, measured steady-state values are averaged across the size range of each bin for low-, medium-, and high-MERV filters. The differences between low- and high-MERV filters and between medium- and low-MERV filters are then calculated in each bin.

Table 2. Description of Indoor and Outdoor Temperature Bins

Entering Wet Bulb, °C (°F)	Outdoor Dry Bulb, °C (°F)							
	23°C–25°C (73°F–77°F)	**25°C–27°C (77°F–81°F)**	**27°C–29°C (81°F–84°F)**	**29°C–31°C (84°F–88°F)**	**31°C–33°C (88°F–91°F)**	**33°C–35°C (91°F–95°F)**	**35°C–37°C (95°F–99°F)**	**37°C–39°C (99°F–102°F)**
17°C–18°C (63°F–64°F)	1	2	3	4	5	6	7	8
18°C–19°C (64°F–66°F)	9	10	11	12	13	14	15	16
19°C–20°C (66°F–68°F)	17	18	19	20	21	22	23	24
20°C–21°C (68°F–70°F)	25	26	27	28	29	30	31	32
	Bin Number (1–32)							

At least 20 measured data points had to be collected in each bin with both filters installed for it to be considered a valid binned comparison. Bins were weighted equally in the analysis.

The final portion of results from the continuous measurements consists of analyzing trends in actual measured energy consumption by the two test systems. Since the thermostat setpoints were precisely controlled during the measurements, we investigated the actual measured change in daily energy consumption in the test systems as a function of only outdoor temperatures. The analysis only compares measurements with high- and low-MERV filters installed in order to have the largest possible dataset for comparison.

RESULTS AND DISCUSSION

The following section details the results from the test system fan curve experiments and from the continuous operation monitoring periods.

Test House Fan Curves

Figure 5 displays the results from the fan curve determination procedure for the two systems in the test house. The curves in Figure 5 present measured fan curves in the same manner as Figure 3 in the background section of this paper.

The results in Figure 5 show that the fan in the upflow test system (Figure 5a) appears to behave somewhat similarly to the hypothetical fan in Figure 3a, and the fan in the downflow system (Figure 5b) behaved similarly to the fan in Figure 3b. However, the pressure, flow, and power relationships show more scatter in the actual measurements than in the hypothetical case. It is important to point out that both Figure 5a (upflow) and 5b (downflow) are plotted on the same vertical and horizontal scales. Although the two systems housed the same air-handler fan, they operated differently. The upflow unit had a steeper fan pressure curve, causing the working points to be located at generally lower airflow rates than the downflow unit. The fan efficiency curve of the upflow unit peaks at a lower value (under 29%) than does the downflow unit (over 32%), although the difference is small and within the uncertainty of the calculation. Peak efficiency occurs at much higher airflow rates and for a longer range of airflows in the downflow unit (approximately 1300-1750 m^3/h or 770–1030 cfm) compared to the upflow unit

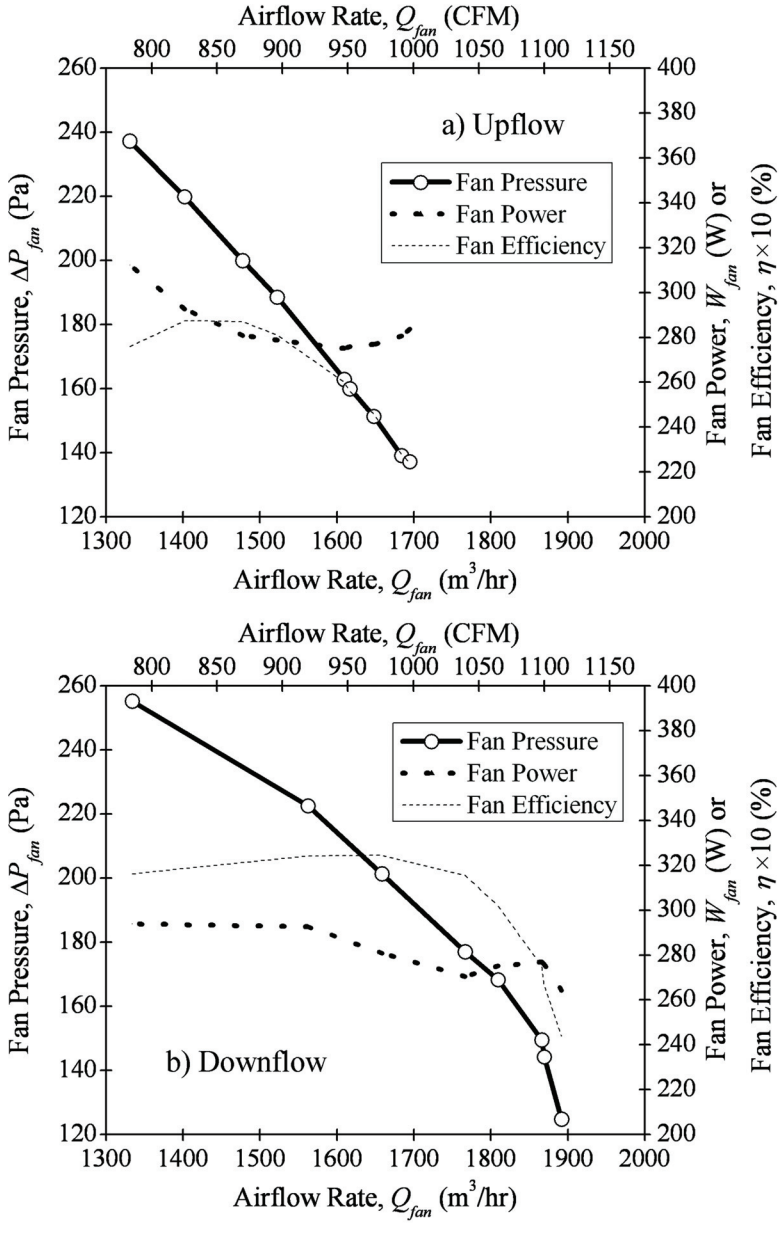

Figure 5. Fan curves for (a) the upflow test system and (b) the downflow test system.

(approximately 1400–1500 m^3/h or 820–880 cfm), suggesting the downward positioning of an identical air-handling unit may result in greater airflow without increasing fan power draw.

The results in Figures 5a and 5b show that an increase in filter efficiency and pressure drop could cause fan power to either increase or decrease in both test house systems, depending upon the working points during actual system operation. For example, as long as a filter does not cause the operating airflow rate to increase or decrease beyond approximately 1500–1650 m^3/h

(880–970 cfm) in the upflow system (Figure 5a), fan power draw will remain constant. In this system, both extremely high and low airflow rates will cause the fan to draw more power. However, if a higher efficiency filter decreases the airflow rate, for example, approximately 15% from 1750 to 1500 m^3/h (1030 to 880 cfm) in the downflow system (Figure 5b), the fan will draw approximately 10% more power.

Continuous Measurements

The following section describes the results of measurements made during the cooling operation periods with low-, medium-, and high-MERV filters. Both systems operated at the same fan speed in cooling and fan-only modes. The next section makes a binned comparison between the values measured with high-MERV filters and low-MERV filters and between values measured with mid-MERV and low-MERV filters. Finally, the last section summarizes the daily energy consumption measured with high- and low-MERV filters installed in the test house.

The results from the continuous cooling operation periods are summarized in Tables 3 and 4. The measured values represent averages taken during steady-state operation, covering the entire life of a filter installation. The uncertainties represent the larger of the standard deviation or instrument uncertainty in the measurements. Table 3 displays measurements related to the filter and air-handling units, while Table 4 describes the performance of the air-conditioning systems, recorded regardless of the effects of climate.

Low-MERV and high-MERV filters were installed for approximately the same amount of time (50+ days), while mid-MERV filters were installed for a considerably shorter amount of time (11 days), as seen in Table 3. This schedule of filter installations was maintained to capture the effects of more extreme changes in filter efficiency. Filter pressure drops showed no observable increase in time and did not vary more than 5 Pa (0.02 in. w.c.) during any filter

Table 3. Filter and Flow Measurements of the Test Systems

System	Filter	Filter Life, days	Filter Pressure Drop, Pa (in. w.c.)	Coil Pressure Drop, Pa (in. w.c.)	Total Fan Pressure, Pa (in. w.c.)	System Airflow, m^3/h (cfm)	AHU Fan Power Draw, W	Efficacy, $(m^3/h)/W$ (cfm/W)
Upflow	Low-MERV	52	25.8±0.3 (0.104±0.001)	57.9±1.3 (0.233±0.005)	162.9±2.2 (0.654±0.009)	1660±80 (980±50)	277±3	6.0±0.4 (3.5±0.2)
	Mid-MERV	11	47.1±0.8 (0.189±0.003)	56.5±1.2 (0.227±0.005)	178.9±3.0 (0.718±0.012)	1610±80 (950±50)	281±3	5.7±0.4 (3.4±0.2)
	High-MERV	51	78.7±0.8 (0.316±0.003)	48.2±1.2 (0.194±0.005)	196.4±1.4 (0.789±0.006)	1550±80 (910±50)	284±3	5.5±0.4 (3.2±0.2)
Down-flow	Low-MERV	52	16.0±2.4 (0.064±0.010)	74.8±0.7 (0.300±0.003)	145.3±2.6 (0.584±0.010)	1720±90 (1010±50)	264±3	6.5±0.5 (3.8±0.3)
	Mid-MERV	11	45.6±0.6 (0.183±0.002)	69.8±1.0 (0.280±0.004)	161.0±3.5 (0.647±0.014)	1580±80 (930±50)	267±3	5.9±0.4 (3.5±0.2)
	High-MERV	51	85.8±0.9 (0.345±0.004)	59.0±0.8 (0.237±0.003)	187.8±1.6 (0.754±0.006)	1530±80 (900±50)	273±3	5.6±0.4 (3.3±0.2)

lifespan, suggesting that minimal dust loading occurred in the unoccupied test house. The pressure drops across mid-MERV filters were approximately 1.9 and 2.9 times larger than that across low-MERV filters in the upflow and downflow units, respectively, while the pressure drops across high-MERV filters were approximately 3 and 5.5 times larger than that across low-MERV filters.

Airflow rates measured with high-MERV filters installed in the upflow and downflow system were 7% and 11% lower, respectively, than that with low-MERV filters installed. The decrease in airflow rates with higher efficiency filters was greater than the 4%–5% increase measured by Parker et al. (1997), but is generally within the range reported by Stephens et al. (2010). Airflow rates measured with medium-efficiency filters were approximately 3% and 8% lower than that with low-efficiency filters installed in the upflow and downflow systems, respectively.

The AHU fans generally behaved in accordance with Figure 5, showing the lowest power draw with low-MERV filters and the highest power draw with high-MERV filters. As filter efficiency increased, fan efficacy (i.e., the amount of volumetric airflow moved by a unit of power) decreased. The pressure rise measured across the fans increased approximately 20% and 30% with high-MERV filters compared to low-MERV filters in the upflow and downflow systems, respectively. If fan efficiencies remained constant, a 20% increase in fan pressure and a 7% decrease in airflow would result in a 12% increase in fan power draw in the upflow system. Similarly, a 30% increase in fan pressure and an 11% decrease in airflow would result in a 16% increase in fan power draw in the downflow system. However, fan efficiencies vary with fan

Table 4. Performance Measurements During Cooling Operation of the Test Systems[1]

System	Filter	Outdoor Temp., °C (°F)	Return Air Wet-Bulb Temperature, °C (°F)	Outdoor Unit Power Draw, W	Sensible Capacity, W (Btu/h)	Latent Capacity, W (Btu/h)	Total Capacity, W (Btu/h)	COP and EER, W/W ((Btu/h)/W)
Upflow	Low-MERV	32.6 (4.4) 90.7 (7.9)	18.6 (0.6) 65.5 (1.1)	1402±16	5250 (320) 17920 (1090)	1280 (200) 4370 (680)	6530 (380) 22290 (1300)	4.0 (0.9) 13.7 (3.1)
	Mid-MERV	32.3 (4.4) 90.1 (7.9)	18.2 (0.5) 64.8 (0.9)	1397±16	5260 (260) 17960 (890)	1280 (180) 4370 (610)	6540 (310) 22330 (1060)	4.0 (0.8) 13.7 (2.7)
	High-MERV	29.8 (4.0) 85.6 (7.2)	17.3 (1.0) 63.1 (1.8)	1280±14	5680 (610) 19390 (2080)	980 (290) 3350 (990)	6660 (670) 22740 (2290)	4.4 (1.0) 15.0 (3.4)
Downflow	Low-MERV	33.1 (4.1) 91.6 (7.4)	19.7 (0.6) 67.5 (1.1)	1853±21	4450 (310) 15190 (1060)	1190 (200) 4060 (680)	5640 (370) 19250 (1260)	2.7 (0.6) 9.2 (2.0)
	Mid-MERV	33.2 (3.9) 91.8 (7.0)	19.4 (0.6) 66.9 (1.1)	1860±21	4210 (310) 14370 (1060)	1120 (190) 3820 (650)	5330 (360) 18200 (1230)	2.5 (0.4) 8.5 (1.4)
	High-MERV	30.4 (3.5) 86.7 (6.3)	18.4 (1.1) 65.1 (2.0)	1749±20	4780 (490) 16320 (1670)	1020 (220) 3480 (750)	5800 (540) 19800 (1840)	2.9 (0.8) 9.9 (2.7)

[1] Numbers in parentheses denote standard deviations. The results in Table 4 do not control for climatic conditions, so variations are due to the combined effects of both filter efficiency and climate. To isloate filter effects, Table 6 presents the results of the binned analysis.

pressure and airflow as seen in Figure 5, so the decreases in airflow and increases in fan pressure combined to increase fan power draw by approximately 3% in both systems with high-MERV filters installed.

Table 4 displays the average performance of the two air-conditioning systems with the three filter efficiencies installed. The measurements are not binned for similar climatic conditions, so the variations are due to the combined effects of both filter efficiency and indoor and outdoor temperatures.

Although the outdoor units were the same size, Table 4 shows that the downflow unit drew approximately 33% more power than the upflow unit, most likely because of the presence of the heat pump and potentially because of different refrigerant charge levels. High-MERV filters were installed during periods of approximately 2°C (3.6°F) lower outdoor temperatures and 1.3°C (2.3°F) lower entering wet-bulb temperatures, on average, than low-MERV filters. The combined effects of climatic conditions, filter efficiencies, and airflow changes caused a 6%–9% decrease in outdoor unit power draw, an 8% increase in sensible capacity, a 15%–25% decrease in latent capacity, a 2%–3% increase in total capacity, and a 7%–10% increase in overall efficiency (COP, EER) with high-MERV filters compared to low-MERV filters. The binned analysis, described below, isolates the effects of filter efficiency by normalizing for similar climatic conditions.

Table 5 describes average airflow and duct leakage measurements made with the different filters installed in the two test systems. The values are averaged over each measured data point and calculated using Equations 4 and 5. Since there were no return ducts in either system, there is no return-side duct leakage, and the reported leakage values are for the supply side only.

The downflow system had more supply-side duct leakage than the upflow system. The upflow system was very tight, with less than 3% of system airflow lost by duct leakage. The downflow system lost approximately 12% of supply airflow by duct leakage. Although the magnitude of supply-side duct leakage airflow generally decreased as filter efficiency increased and airflow rates decreased, the fraction of duct leakage to system airflow did not change.

Figure 6 displays pressure distribution diagrams for the two test systems, averaged with high- and low-MERV filters installed. Filters were located at the return side of the AHU, but because there are no return ducts, this pressure distribution diagram is not directly comparable to the system represented in Figure 4 in the background section. The test systems thus cannot offer insight into changes in return duct leakage likely due to high-pressure-drop filters.

The total pressure rise across the fan increased in both systems with high-MERV filters installed compared to low-MERV filters, which, when combined with airflow changes, moved the working point along the fan power curve to increase fan power draw a small amount. The total pressure rise across the fan increased approximately 20% in the upflow system and approximately 30% in the downflow system with high-MERV filters installed. The decreases in supply operating pressure of approximately 13% in the upflow system and 20% in the downflow system with high-MERV filters relate directly to the measured decreases in airflow and supply leakage flow. Coil pressure drops decreased approximately 17% in the upflow system and approximately 21% in the downflow system with high-MERV filters.

Binned Analysis. To separate climatic effects from filter effects in the test systems, Table 6 shows the results of the binned analysis (bins are described in Table 2). This analysis shows the effect of rated filtration efficiency on operational parameters related to energy consumption recorded during similar climatic conditions in the cooling mode. Table 6 compares both high-MERV filters to low-MERV filters, and mid-MERV filters to low-MERV filters. Reported values are the mean percentage differences in a given parameter, averaged first over each data point recorded in a particular bin, then averaged across all bins. The values in each bin were

average values measured during steady-state operation with each type of filter installed. The percentage differences for values measured with high- and mid-MERV filters are compared to those measured with low-MERV filters. Negative values mean that the measured parameter was lower with a high- or mid-MERV filter, and positive values mean high- or mid-MERV filters increased the parameter.

The binned analysis should isolate any climatic effects by comparing each parameter at similar indoor and outdoor environmental conditions. Similar to the previous results, fan power draw increased approximately 3%–4% in the test systems with high-MERV filters compared to low-MERV filters, and increased approximately 0%–2% with mid-MERV filters compared to low-MERV filters. High-MERV filters reduced the power draw of the outdoor unit by less than 1% in both systems, and medium-MERV filters increased the outdoor unit power draw by less than 1% in both systems. The net effect on total power draw (i.e., fan + outdoor unit power draw) was less than 1% in both systems with both medium- and high-efficiency filters.

The binned analysis shows that the supply leakage airflow rate decreased approximately 9%–11% with high-MERV filters, and 3%–7% with medium-MERV filters, although because system airflow rates also decreased, no change was seen in leakage fraction. Sensible, latent, and

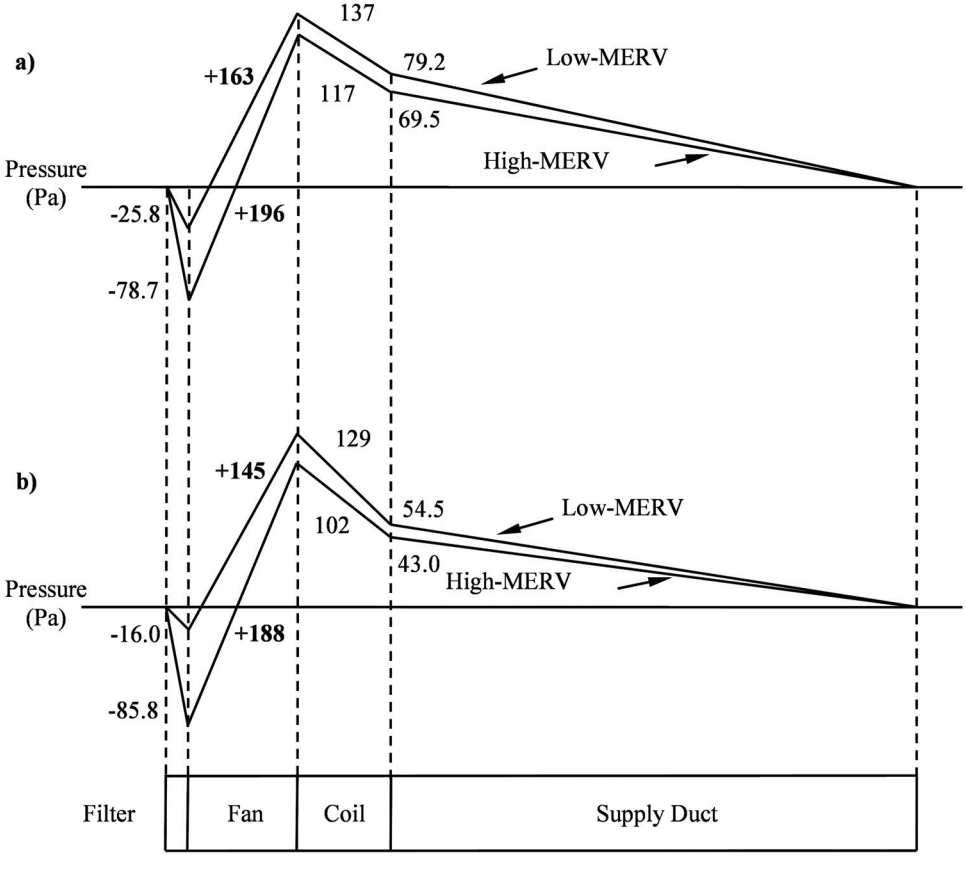

Figure 6. Pressure distribution with high- and low-MERV filters in (a) the upflow system and (b) the downflow system.

Table 5. Duct Leakage Measurements for the Test Systems

System	Filter Efficiency	System Airflow, m^3/h (cfm)	Supply Leakage to Exterior, m^3/h (cfm)	Supply Leakage Fraction, %
Upflow	Low	1660±80 (980±50)	37±2 (22±1)	2.2% ± 6%
	Medium	1610±80 (950±50)	36±2 (21±1)	2.2% ± 6%
	High	1550±80 (910±50)	34±2 (20±1)	2.2% ± 6%
Downflow	Low	1720±90 (1010±50)	197±6 (116±4)	11.4% ± 6%
	Medium	1580±80 (930±50)	183±6 (108±4)	11.6% ± 6%
	High	1530±80 (900±50)	178±5 (105±4)	11.6% ± 6%

Table 6. Binned Comparison Results During Cooling Mode Operation

Measured Parameter[1]	Upflow System		Downflow System	
	High vs. Low	Medium vs. Low	High vs. Low	Medium vs. Low
Fan power draw	+3.3%	+2.1%	+4.0%	+0.5%
Outdoor unit power draw	−0.8%	+0.5%	−0.1%	+0.6%
Total power draw	−0.1%	+0.8%	+0.4%	+0.5%
System airflow	−6.8%	−2.9%	−10.9%	−8.4%
Supply leakage airflow	−8.4%	−3.0%	−9.4%	−6.8%
Temperature difference across coil	+4.5%	+0.5%	+7.8%	+0.7%
Humidity ratio difference across coil	+1.5%	+9.7%	+8.5%	+9.8%
Sensible capacity	−2.6%	−2.5%	−4.0%	−8.0%
Latent capacity	−5.5%	+6.5%	−3.3%	−0.1%
Total capacity	−3.1%	−0.8%	−3.8%	−6.4%
COP (EER)	−3.1%	−2.0%	−4.2%	−7.3%

[1] Table 6 reports average differences measured with high-MERV filters compared to low-MERV filters, and medium-MERV filters compared to low-MERV filters. The differences are first averaged during steady-state operation period in each bin.

total capacity decreased approximately 3%–6% with high-MERV filters installed compared to low-MERV filters and had more scattered effects with medium-MERV filters installed. Capacity reductions were linked largely to airflow reductions because both temperature and absolute humidity differences across the cooling coil actually increased in the presence of high-MERV and mid-MERV filters (refer to Equation 6 for capacity calculations). The net effect of high-MERV filters was approximately a 3% decrease in system efficiency in the upflow system and a 4% decrease in system efficiency in the downflow system. The decreases in efficiency are similar to those predicted in the background section and similar to those reported in the literature due to a 5%–10% airflow reduction (Palani et al. 1992; Rodriguez et al. 1996; Parker et al. 1997; Kim et al. 2009) and are smaller than the changes attributable to varying climate conditions (see Table 4). The net effect of medium-MERV filters was approximately a 2% decrease in system efficiency in the upflow system and a 7% decrease in system efficiency in the downflow system. The discrepancy in efficiency measured in the two test systems with medium efficiency filters suggests that the effects of higher pressure drop filters are not entirely predictable.

Although changes in capacity and efficiency were measured between filter installations in the test house data, the magnitudes are generally small and often within propagated instrument uncertainty. The total power draw and sensible capacity results suggest that the test systems drew about the same amount of power with higher-efficiency filters as low-efficiency filters, but had to run 2%–4% longer to meet the cooling load with high-MERV filters, and 2%–8% longer with medium-MERV filters. However, little is known about how the measure of sensible capacity actually affects thermostat readings and system runtime in real environments. Since the thermostat setpoints were precisely controlled during the measurements, we investigated the actual measured change in daily energy consumption in the test systems with high- and low-MERV filters only as a function of average daily outdoor temperature. Only high- and low-MERV filters are used in this analysis because the extended monitoring times provided more data than the medium-MERV tests. Figure 7 compares the daily energy consumption recorded in the two test systems with high- and low-MERV filters installed. The data points in Figure 7 are taken only during overlapping average daily outdoor temperature ranges (between 25°C [77°F] and 30°C [86°F]) and only during days when 24 hours of data were recorded. This provides data for 24 full days with low-MERV filters installed and 16 full days with high-MERV filters installed to compare daily energy consumption. A linear regression is performed across the outdoor temperature range and the 95% confidence interval is displayed in Figure 7.

The difference in the 95% confidence intervals of the regressions of daily energy consumption with low-MERV filters and high-MERV filters are not statistically significant for either test house system, suggesting that high-efficiency filters did not cause the test systems to use more energy. Although energy consumption can be affected by environmental factors other than the ones for which we controlled (e.g., solar radiation, wind speed, or temporal distribution of outdoor temperatures), both the scatter and overlapping relationships for low- and high-MERV filters show that there was no significant change in daily energy consumption in the test systems due to high-efficiency filters. Thus, both the small differences and the directional variations in regression slopes with high- and low-efficiency filters in the two test systems suggest that the energy consequences of high-efficiency filters were not only small but also unpredictable.

This paper is a companion to Stephens et al. (2010), which describes similar measurements that took place over a year on 17 HVAC systems in occupied residential and light-commercial buildings. The results from that work generally show similar findings related to pressure, flow, and power draw measurements with similar types of filters as this study, albeit with considerable

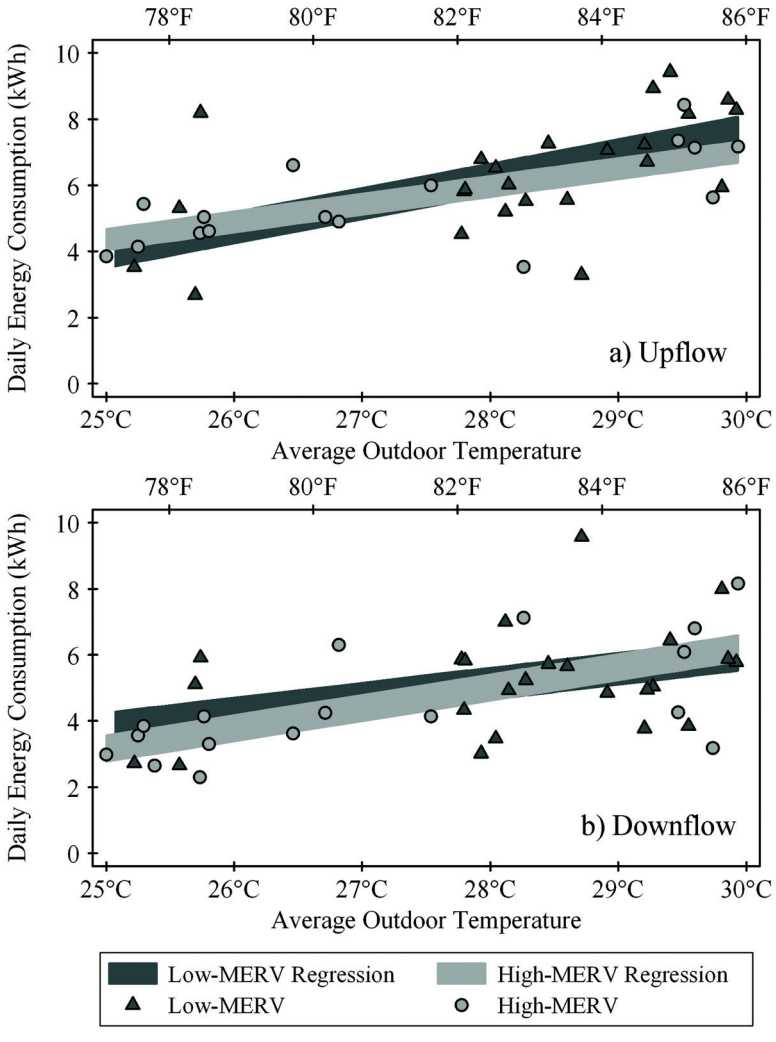

Figure 7. Daily energy consumption with high- and low-MERV filters in (a) the upflow system and (b) the downflow system.

variation that is typical of field studies. Changing climatic and operating conditions caused a large amount of scatter in the companion field study that we were able to control in this study.

To summarize, the primary findings of this experimental investigation of the two test systems include the following.

- High-MERV filters decreased airflow rates by approximately 7% and 11% in each of the two systems, relative to low-MERV filters.
- Mid-MERV filters decreased airflow rates by approximately 3% and 8% in each of the two systems, relative to low-MERV filters.
- Fan power draw increased approximately 3%–4%, and the power draw of the outdoor unit decreased less than 1% in the presence of high-MERV filters compared to low-MERV filters.

- Fan power draw increased between 0%–2%, and power draw of the outdoor unit decreased less than 1% in the presence of mid-MERV filters compared to low-MERV filters in one system and increased less than 1% in the other.
- Total capacity and system efficiency decreased approximately 3%–4% in the presence of high-MERV filters.
- Total capacity and system efficiency decreased approximately 1%–2% in one system and approximately 6%–7% in another system in the presence of mid-MERV filters.
- Daily energy consumption did not significantly differ between low- and high-MERV filter installations.

CONCLUSION

Smaller residential HVAC systems behave differently than large commercial systems with flow controls, and the energy consequences of higher efficiency (higher pressure drop) filters are less predictable. A review of the underlying theory behind pressure drop and flow relationships in smaller systems indicates that the energy consequences of higher pressure drop filters are likely small. Furthermore, our experimental verification conducted on two residential air-conditioning systems assesses the magnitude of energy consequences with three levels of high-efficiency filters: low-efficiency fiberglass panel filters (MERV < 4), medium-efficiency synthetic pleated filters (MERV 8), and high-efficiency synthetic pleated filters (MERV 11). The results herein suggest that high-efficiency filters did not have much of an impact on energy consumption in residential air-conditioning test systems and that other factors should govern filter selection.

ACKNOWLEDGMENTS

We would like to extend thanks to the members of the RP-1299 Project Monitoring Subcommittee for their helpful review of this work. The American Society of Heating, Refrigerating and Air-Conditioning Engineers (ASHRAE), the National Science Foundation (IGERT Award DGE #0549428), and an ASHRAE Graduate Student Grant-in-Aid provided funding for this research.

REFERENCES

ASHRAE. 2004a. Chapter 16, "Duct Construction." *2004 ASHRAE Handbook—HVAC Systems and Equipment*. Atlanta: American Society of Heating, Refrigerating and Air-Conditioning Engineers, Inc.

ASHRAE. 2004b. Chapter 18, "Fans." *2004 ASHRAE Handbook—HVAC Systems and Equipment*. Atlanta: American Society of Heating, Refrigerating and Air-Conditioning Engineers, Inc.

ASHRAE. 2004c. *ANSI/ASHRAE Standard 152-2004, Method of Test for Determining the Design and Seasonal Efficiencies of Residential Thermal Distribution Systems*. Atlanta: American Society of Heating, Refrigerating and Air-Conditioning Engineers, Inc.

ASHRAE. 2005. Chapter 35, "Duct Design." *2004 ASHRAE Handbook—HVAC Systems and Equipment*. Atlanta: American Society of Heating, Refrigerating and Air-Conditioning Engineers, Inc.

ASHRAE. 2007. *ANSI/ASHRAE Standard 52.2-2007, Method of Testing General Ventilation Air-Cleaning Devices for Removal Efficiency by Particle Size*. Atlanta: American Society of Heating, Refrigerating and Air-Conditioning Engineers, Inc.

Chan, W., W. Nazaroff, P. Price, M. Sohn, and A. Gadgil. 2005. Analyzing a database of residential air leakage in the United States. *Atmospheric Environment* 39(19):3445–55.

Chimack, M., and D. Sellers. 2000. Using extended surface air filters in heating ventilation and air conditioning systems: Reducing utility and maintenance costs while benefiting the environment. In the *Proceedings of the 2000 ACEEE Summer Study on Energy Efficiency in Buildings* 3:77–88.

Downey, T., and J. Proctor. 2002. What can 13,000 air conditioners tell us? In the *Proceedings of the 2002 ACEEE Summer Study on Energy Efficiency in Buildings* 1:53–67.

Fisk, W., D. Faulkner, J. Palonen, and O. Seppanen. 2002. Performance and costs of particle air filtration technologies. *Indoor Air* 12(4):223–34.

Francisco, P., J. Siegel, L. Palmiter, and B. Davis. 2006. Measuring residential duct efficiency with the short-term coheat test methodology. *Energy and Buildings* 38:1076–83.

HUD. 2005. American Housing Survey for the United States: 2005. US Department of Housing and Urban Development.

Kim, M., W. Payne, P. Domanski, S. Yoon, and C. Hermes. 2009. Performance of a residential heat pump operating in the cooling mode with single faults imposed. *Applied Thermal Engineering* 29:770–78.

O'Neal, D., A. Rodriguez, M. Davis, and S. Kondepudi. 2002. Return air leakage impact on air conditioner performance in humid climates. *Journal of Solar Energy Engineering* 124:63–69.

Palani, M., D. O'Neal, and J. Haberl. 1992. The effect of reduced evaporator air flow on the performance of a residential central air conditioner. In the *Proceedings of the 1992 Symposium on Building Systems in Hot-Humid Climates*, pp. 20–26.

Parker, D., J. Sherwin, R. Raustad, and D. Shirey, III. 1997. Impact of evaporator coil airflow in residential air-conditioning systems. *ASHRAE Transactions* 103(2):395–405.

Proctor, J., and D. Parker. 2000. Hidden power drains: Residential heating and cooling fan power demand. In the *Proceedings of the 2000 ACEEE Summer Study on Energy Efficiency in Buildings* 1:225–34.

Rodriguez, A., D. O'Neal, M. Davis, and S. Kondepudi. 1996. Effect of reduced evaporator airflow on the high temperature performance of air conditioners. *Energy and Buildings* 24:195–201.

Sachs, H., T. Kubo, S. Smith, and K. Scott. 2002. Residential HVAC fans and motors are bigger than refrigerators. In the *Proceedings of the 2002 ACEEE Summer Study on Energy Efficiency in Buildings* 1:261–72.

Sherman, M. 2008. Infiltration in ASHRAE's residential ventilation standards. LBNL 1220E. Lawrence Berkeley National Laboratory, Berkeley, CA.

Siegel, J., I. Walker, and M. Sherman. 2000. Delivering tons to the register: Energy efficient design and operation of residential cooling systems. In the *Proceedings of the 2000 ACEEE Summer Study on Energy Efficiency in Buildings* 1:295–306.

Stephens, B., J. Siegel, and A. Novoselac. 2010. Energy implications of filtration in residential and light-commercial buildings (RP-1299). *ASHRAE Transactions* 116(1).

The Energy Conservatory. 2006. *TrueFlow® Air Handler Flow Meter Operation Manual.* Minneapolis, MN: The Energy Conservatory.

The Energy Conservatory. 2007. *Minneapolis Duct Blaster® Operation Manual*. Minneapolis, MN: The Energy Conservatory.

Walker, I., J. Siegel, K. Brown, and M. Sherman. 1998. Saving tons at the register. In the *Proceedings of the 1998 ACEEE Summer Study on Energy Efficiency in Buildings* 1:367–84.

Waring, M., and J. Siegel. 2008. Particle loading rates for HVAC filters, heat exchangers, and ducts. *Indoor Air* 18(3):209–24.

Yang, L., J. Braun, and E. Groll. 2007. The impact of evaporator fouling and filtration on the performance of packaged air conditioners. *International Journal of Refrigeration* 30(3):506–14.